

Crosswell reflection imaging

Guoping Li and Robert R. Stewart

ABSTRACT

A processing flow for crosswell seismic imaging with reflections is presented in this paper. It is composed of steps such as data gathering, wavefield separation, velocity analysis, moveout corrections, and stack in common reflection bin gathers. Four types of data domains, including common-shot, common-receiver, common-interval, and common-mid-depth gathers, are used for different processing purposes. Direct arrivals are removed in common-interval gathers. Reflection wavefield separation is performed in common-shot gathers. The data are corrected for vertical and horizontal moveouts in common-mid-depth gathers, with velocity information derived from a zero-interval gather. Reflection data are finally stacked in common reflection bin gathers to yield a final image. The whole processing procedure is very similar to CDP processing of surface seismic reflection data. The advantage of multi-fold coverage of crosswell seismic data is fully utilized. We will conceptually demonstrate the processing steps with a synthetic crosswell data example numerically generated from a constant-velocity medium.

INTRODUCTION

Traditionally, crosswell seismic data have been used to tomographically image the subsurface seismic velocity variation in a region between wells. Most tomographic imaging methods are based using direct wave traveltimes. Crosswell direct arrivals represent only a small fraction of the total seismic information recorded in crosswell data, so a velocity picture tomographically inverted generally is not good enough for detailed reservoir delineation and characterization (Baker and Harris, 1984). The horizontal resolving power provided by direct arrival traveltime tomographic inversion is limited by the limited angular ray coverage of a crosswell geometry (Menke, 1984). In particular, tomographic inversion cannot image geological formations below borehole depths, where meaningful reservoirs may be located.

Over the last decade, a few studies discussing crosswell reflection processing have appeared in the geophysics literature. Early work of Baker and Harris (1984) and Iverson (1988) first reported the use of reflections in crosswell imaging. Following them, Abdalla et al. (1990) and Lazaratos et al. (1991) studied kilohertz crosswell seismic reflection data. These studies extracted later arriving reflection events from the whole complex wavefield through effective processing. The extracted reflected waves are used to image the region between wells. To obtain an image from crosswell reflection data, they all used a VSP-CDP mapping algorithm which Wyatt and Wyatt (1984) developed to process VSP data. The result of imaging with crosswell reflection data has been found to be greatly improved. For real crosswell data in a frequency range of several kilohertz, a vertical resolution of a few feet can be obtained (Iverson, 1988; Abdalla et al., 1990; and Lazaratos et al., 1991).

However, a problem with the previous crosswell reflection imaging methods is that, since they derive a depth image from a single shot (or receiver) gather only, the lateral coverage obtained is vary limited --- usually only a small portion of the

subsurface reflectors between wells can be imaged. This is explained in the crosswell coverage map given by Abdalla et al. (1990). Hence, if such processing methods are used for crosswell reflection imaging, multi-fold coverage provided by modern crosswell acquisition configurations will not be fully used. Obviously a more general method for crosswell reflection processing and imaging is needed.

Today's surface reflection seismic method is mature. This mature method is characterized by CDP-based data processing techniques. Multiple data domains, namely, common-shot gather, common-receiver gather, common-offset gather, and common depth point (CDP) gather, are often used for various processing purposes. More importantly, CDP processing techniques sort seismic trace data from common-shot (or receiver) gathers into CDP gathers so that redundancy due to multifold coverage of single reflection points is achieved. Because of such redundancy, reflection signals from the same subsurface points are best enhanced while various kinds of noises are reduced to a statistically satisfying degree.

It has been hoped that crosswell seismic reflection data can be processed in a manner more akin to the mature CDP data processing procedure. Towards this goal, efforts have been made by various geophysical workers during last a few years. Stewart and Machisio (1991) presented a physical model crosswell reflection study. In this study, they first proposed a method of CDP type imaging with multi-fold crosswell data. The method was developed from the idea described by Stewart et al. (1991). Some modification was made by Li and Stewart (1992).

In this paper, we describe a modified procedure of crosswell seismic reflection data. This imaging procedure consists of several main steps such as data gathering, wavefield separation, velocity analysis, moveout corrections, and stack in common reflection bin gathers. Reflection signals are extracted from every data gather available. Four types of data domains are used, including common-shot, common-receiver, common-interval, and common-mid-depth gathers. Direct arrivals are removed in common-interval gathers. Reflection wavefield separation is performed in common-shot gathers. The data are corrected for vertical and horizontal moveouts in common-mid-depth gathers, with velocity information derived from a zero-interval gather. Reflection data are finally stacked in common reflection bin gathers to yield a final image. We will conceptually demonstrate these important processing steps with a synthetic crosswell data example numerically generated from a constant-velocity medium.

FUNDAMENTALS

Synthetic data description

Using a constant-velocity medium, P-wave direct and reflected arrivals were ray traced by using a seismic numerical modeling software. To generate synthetic crosswell seismic data, a crosswell geometry as shown in Figure 1 is used. The well-to-well separation distance is 500 m. 40 explosive-type sources, whose depths range from 20 m to 800 m at an interval of 20 m, are shot in the source well. Positioned in the receiver well are 80 hydrophones each spaced at 10 m from 10 m to 800 m in depth. The constant-velocity earth model was composed of a horizontally flat reflector 850 m deep, separating the medium into two half spaces. The upper half space has a velocity of 2500 m/s, and in the lower half space, the velocity is 3800 m/s.

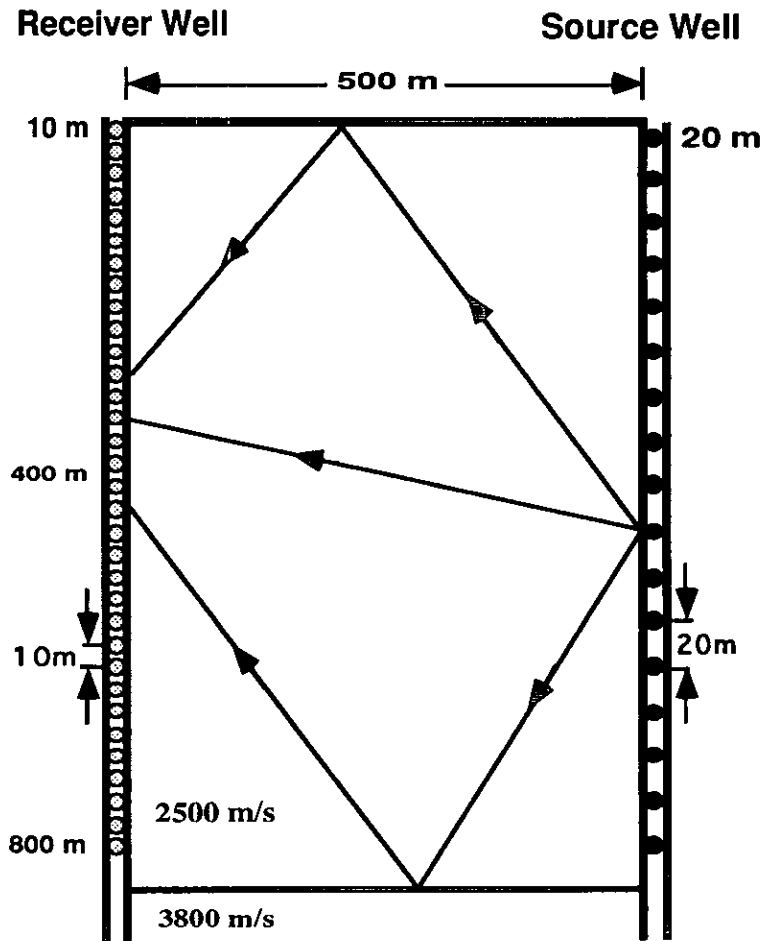


FIG. 1. Crosswell surveying geometry and a constant-velocity earth model with a flat reflector at depth of 850 m. Well-to-well separation distance is 500 m. 40 sources are shot from 20 m to 800 m at 20 m intervals. Receivers are located at depths of 10 m to 800 m at spacing of 10 m.

A total of 40 shot records, each having 80 traces, were recorded. The record length is 1000 ms with a sampling interval of 1.0 ms. A 40 Hz zero-phase Ricker wavelet was used, whose length was 60 ms. The data were recorded in SEG-Y format. The Inverse Theory & Application (ITA) interactive seismic processing software was used in much of the processing of the data.

Figure 2 shows two example shot records from source depths of 200 m (left) and 400 m (right), respectively. On both records, a P-wave direct arrival shows a hyperbolic pattern. Two reflection events, one from the deep reflector and the other from the surface reflector, are seen to have moveouts with opposite dips. Notice the phase change of both direct and reflected waves. They are caused by the change in emergence angle, with respect to the vertical well, of raypaths from each source-receiver pair during raytracing. Although a wavelet shaping filter could have been applied to remove the phenomena, we left the waveforms of the data unchanged to show their effect on our final imaging result.

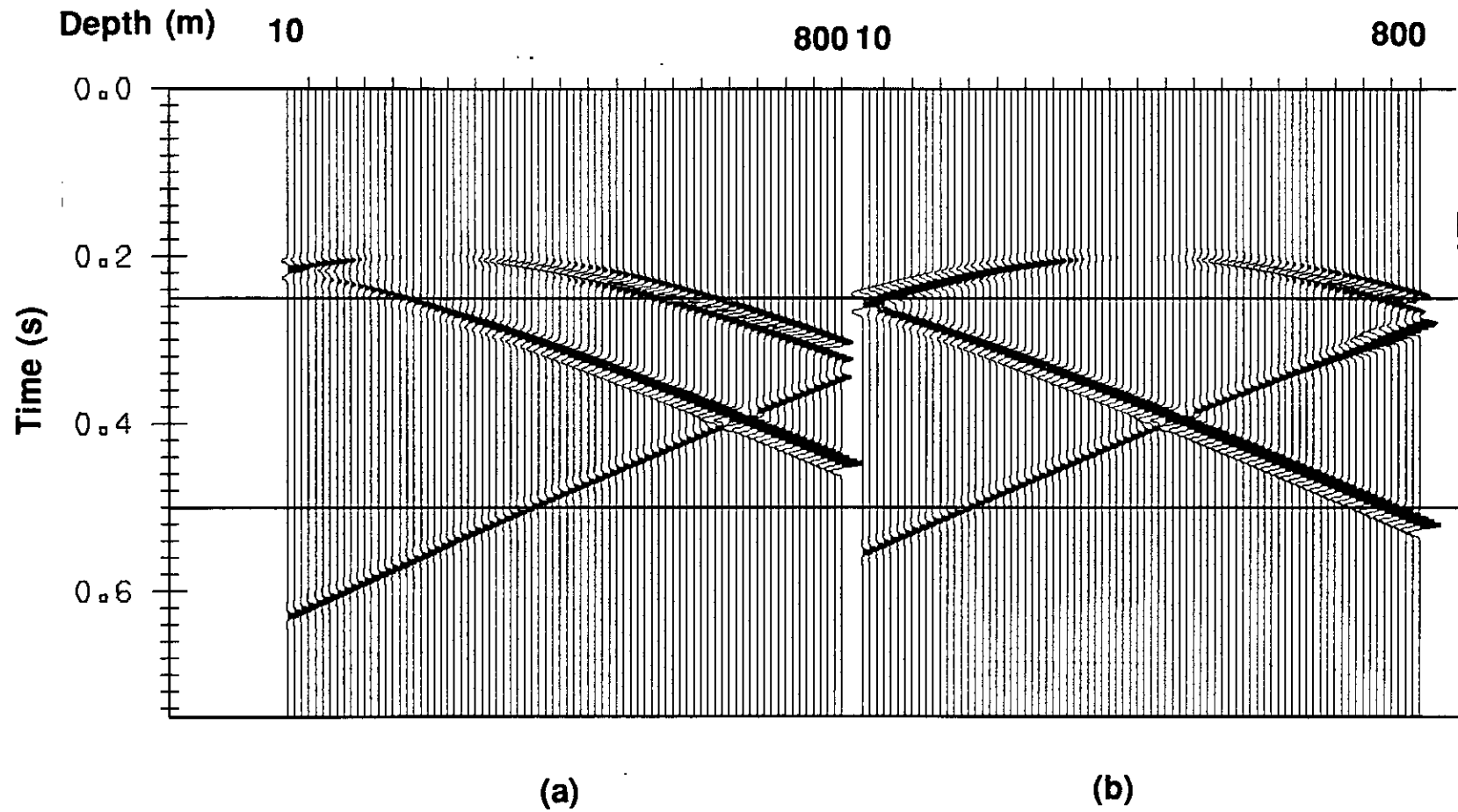


FIG. 2 Common shot gathers of synthetic crosswell data numerically generated from the earth model in FIG. 1. Source depth is 200 m (a) and 400 m (b). A total of 80 receivers are used. Their depths are from 10 m to 800 m at spacing of 10 m.

Data gathering domains

As we have said before, our crosswell reflection imaging procedure is based on multiple data gathering domains. The domains that can be used include common-shot gather, common-receiver gather, common-interval (or offset) gather, and common-mid-depth gather. For simplicity, short forms, CS for common-shot, CR for common-receiver, CI for common-interval, and CMD for common-mid-depth, will be adopted in this paper, respectively. Figure 3 shows a schematic diagram of these four gathers.

Common-shot or common-receiver gathering is not a new idea. In fact, they often represent a natural data format of collecting traces during a field data acquisition process. We have shown examples of CS gathers in Figure 2. Four CR gathers of the synthetic crosswell data are given in Figure 4, where both direct and reflected arrivals have a very similar feature to those in common-shot gathers. A common-shot or common-receiver gather comprises a starting point for VSP-CDP type crosswell reflection imaging methods which were described above.

A common-interval gather is a collection of those traces whose vertical intervals between depths of all related source-receiver pairs are constant (see Figure 3). In a constant velocity medium, the source-to-receiver distance is a straight line. Therefore, direct arrivals from each source-receiver pair have the same traveltimes. In other words, direct arrivals are a flat event in CI gathers. This is confirmed in Figure 5 where several synthetic CI gathers are displayed. Perfectly aligned direct wave events are seen above reflections. Upgoing and downgoing reflections have positive and negative time dips. Notice that both upgoing and downgoing reflections have a very sharp contact with the direct arrival event, an important characteristic of CI gathers. CI gathers can be used to remove direct arrivals (both P and S waves), which will be discussed later. For real crosswell data, direct arrivals in CI gathers may give indications of velocity change with depth.

In a CMD gather, traces are collected for those source-receiver pairs whose sum of depths is constant (refer to Figure 3). So in such a gather energy reflected from a flat layer in a constant velocity medium will have the same traveltimes for all traces, that is, reflections will become flat in a CMD gather. Figure 6 shows six common mid-depth gathers from 6 different CMD depths. In each of them, reflections from the deep reflector (upgoing) and from the surface reflector (downgoing) both are flat, while the direct arrival is symmetrically hyperbolic in pattern. It is also noted that the traveltimes of reflection events from the same reflectors varies from gather to gather, implying the existence of so-called vertical moveout. We will discuss this later. CMD gathers provide partial images of reflectors, can be used as an intermediate step to enhance the reflected arrivals, or be a starting point for a mapping procedure (Stewart, 1991). Besides, flatness of reflection events in CMD is meaningful in real data case. It may indicate 1) whether or not the actual medium being considered is homogeneous or closely homogeneous; 2) whether or not reflectors in the medium, if homogeneous or nearly homogeneous, are flat.

Figure 7 depicts the relationship among the coordinates used in these four data transformation domains. A crosswell stacking chart (Figure 8) is provided by Stewart (1991) to view the types of gathers and their fold. This chart is similar, in many aspects, to the stacking chart used in surface seismic data, for example, as given by Yilmaz (1987).

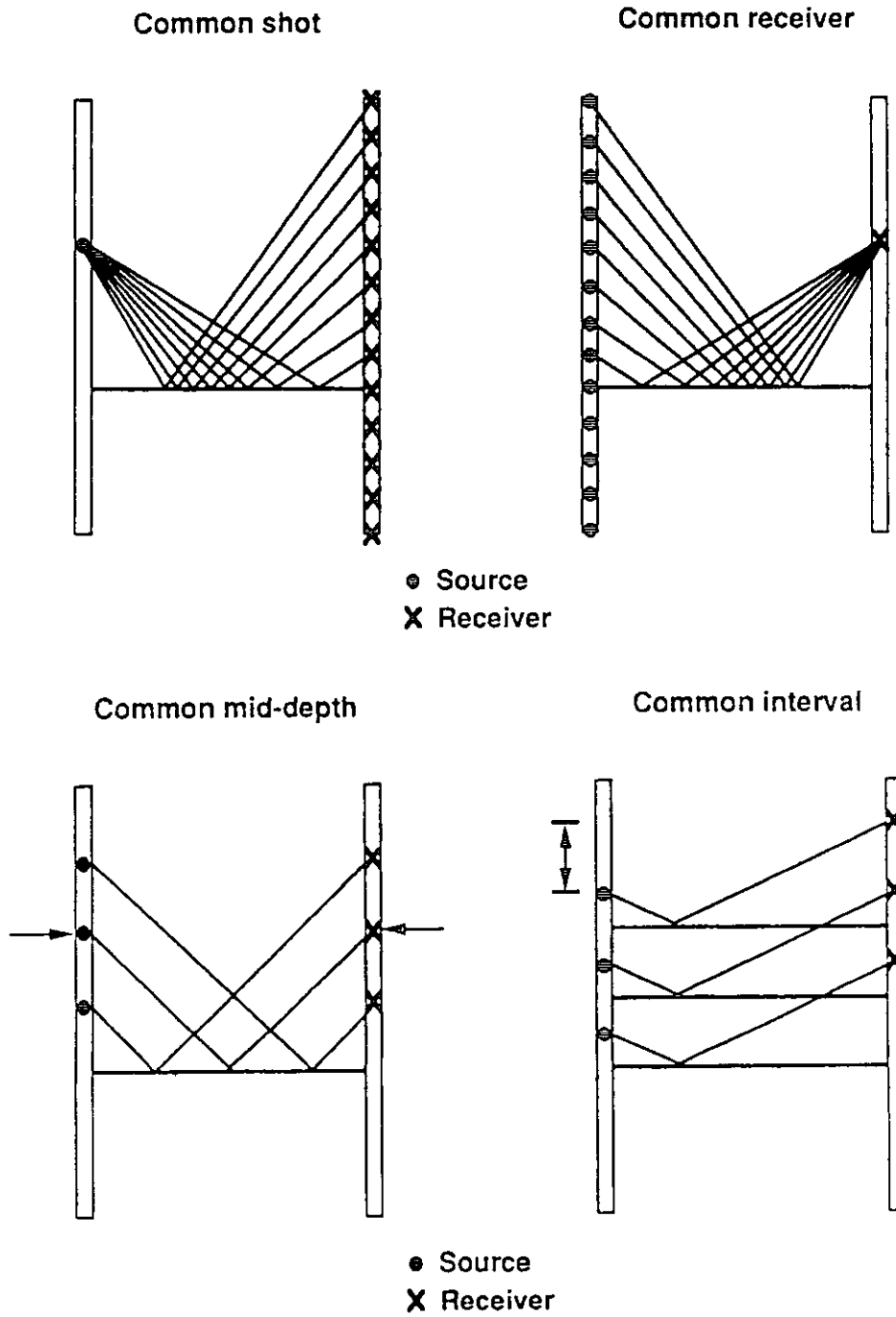


FIG. 3. Four types of data gathering in the crosswell geometry (after Stewart, 1991).

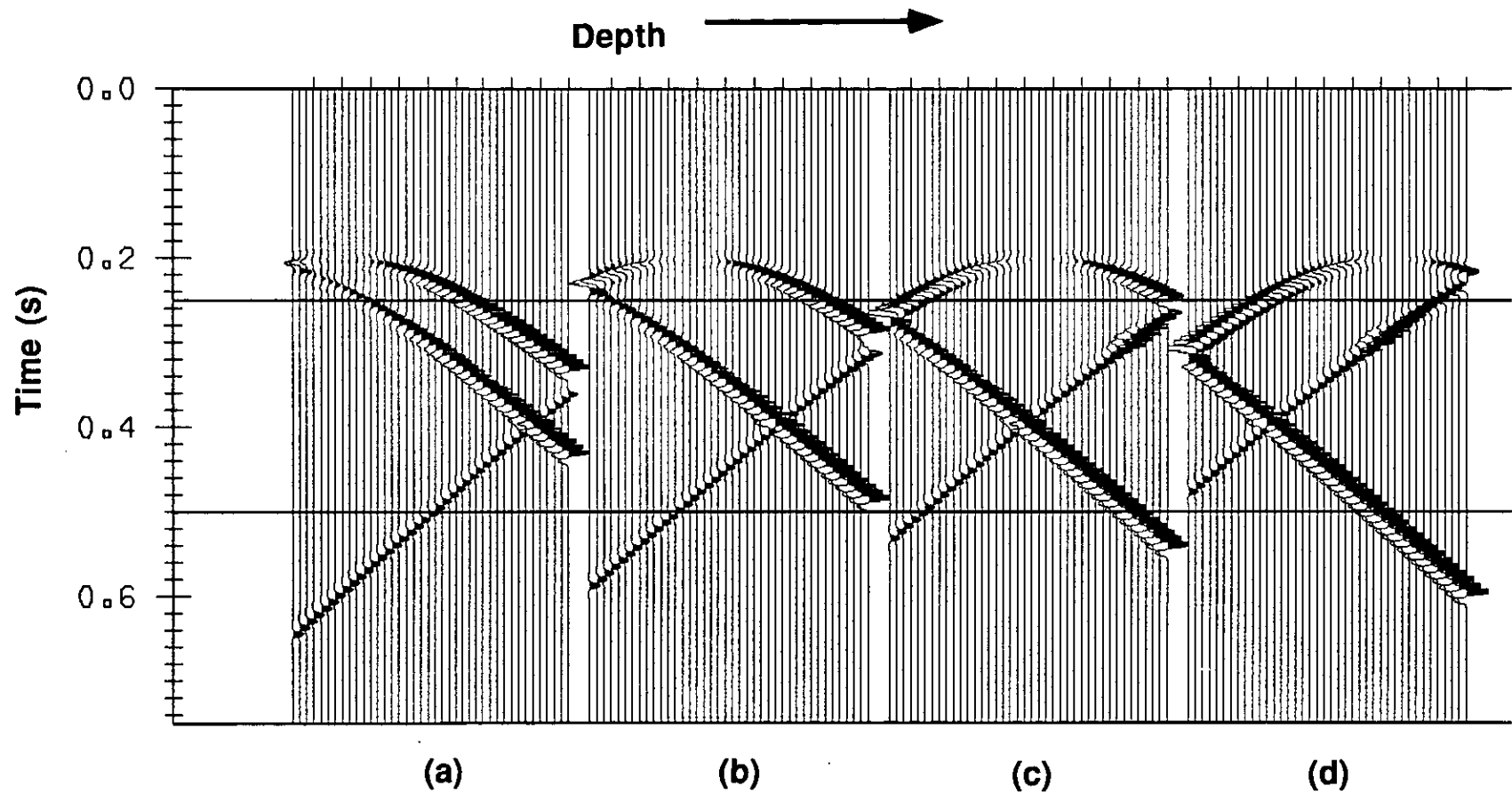


FIG. 4. Four common receiver gathers. The receiver depth is at 150 m (a), 300 m (b), 450 m (c) and 600 m (d), respectively. From left to right, sources are shot from shallow (20 m) to deep (800 m), at intervals of 20 m.

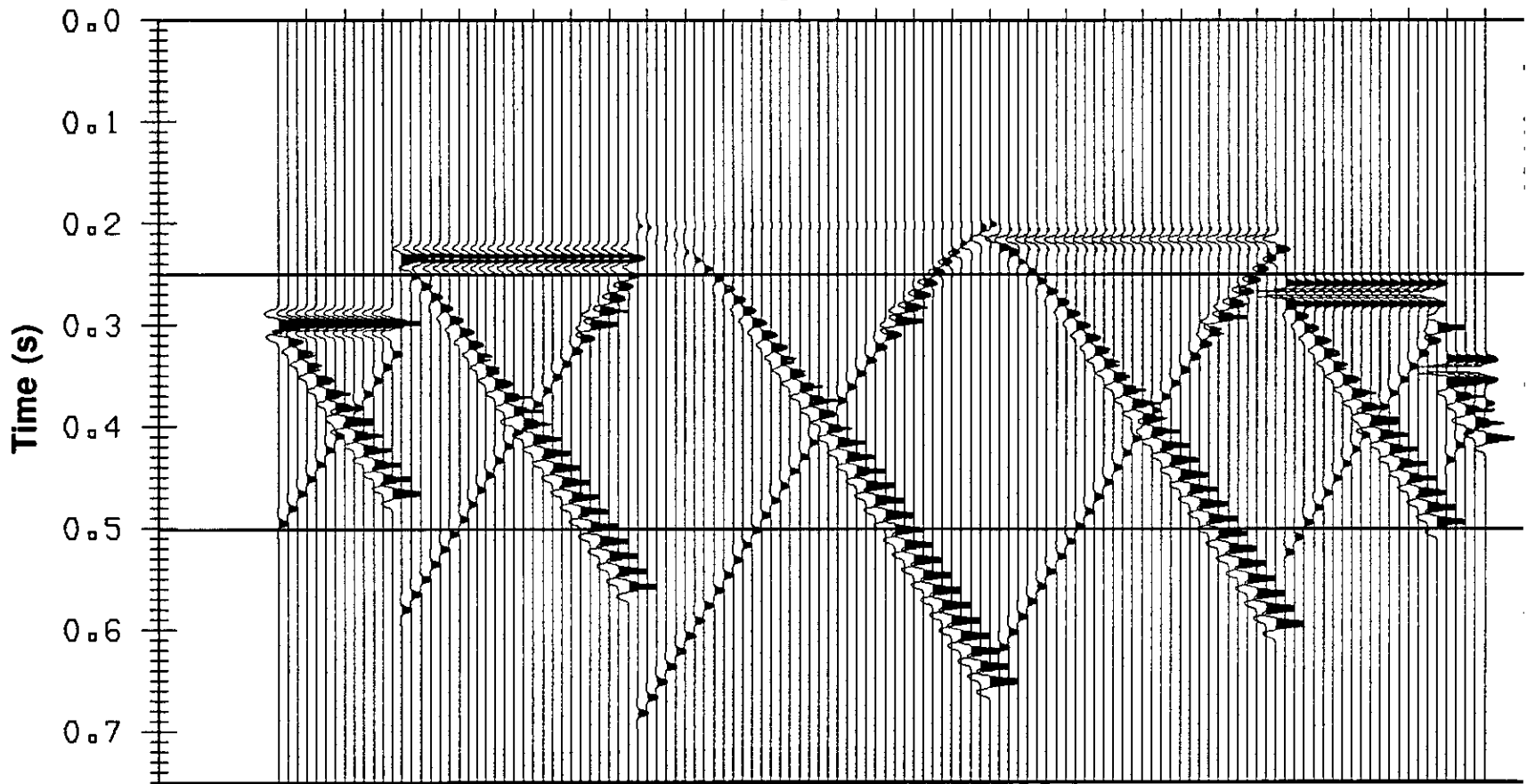


FIG. 5. Common interval gathers. Direct arrival is flat. Upgoing and downgoing reflections have opposite dips. The gathers which have smaller vertical intervals between the source and receiver depths have more traces.

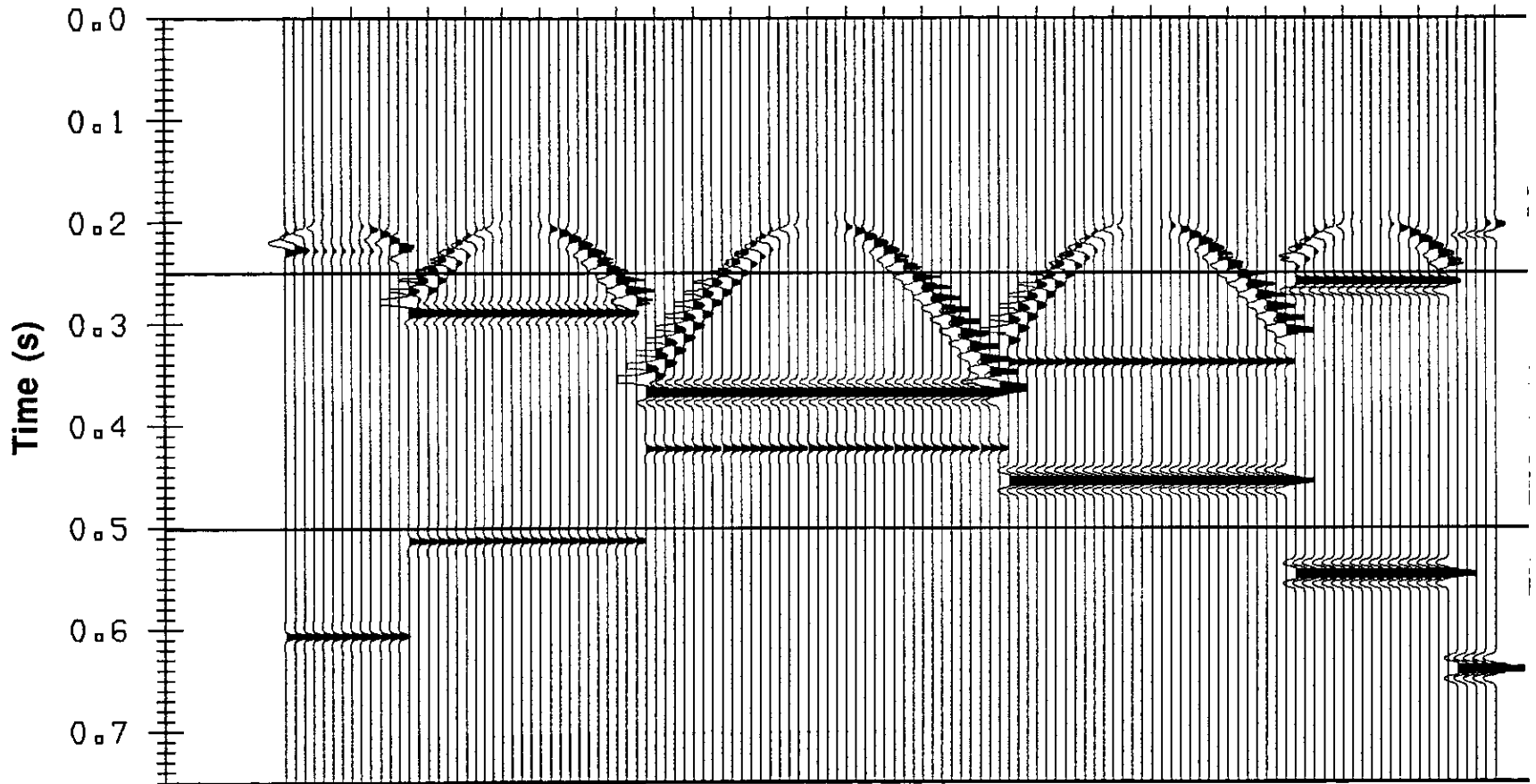


FIG. 6. Common mid-depth gathers. The hyperbolic events are direct arrival waves. Both upgoing and downgoing reflection become flat. When CMD depth gets closer to the middle of a recording spread, there will be more traces in the CMD gather corresponding to that depth.

Processing flow

A processing flow is developed for crosswell reflection processing and imaging based on the use of multiple data domain (Figure 9). As shown in the flow, the whole processing procedure is composed of four major parts. They are: preprocessing, wavefield separation, velocity analysis and moveout corrections, and stacking. Many of the processing steps are performed in different data gathers. A detailed description of each processing step except preprocessing will be given in the subsequent sections.

WAVEFIELD SEPARATION

The idea of separating upgoing and downgoing wave modes in crosswell seismic data stems from VSP data processing. It forms an important processing step in the whole imaging procedure (Figure 9). The wavefield contained in borehole seismic data often is very complex. In the VSP case, data usually are composed of compressional and shear transmitted waves (downgoing direct arrivals), P and S upgoing primary reflections and their multiples, as well as many other wave modes (such as tube waves), and noises. Except primary reflections and direct arrivals, which are often useful wave modes in VSP data processing, all the rest of the wavefield is regarded as unwanted waves. VSP data are processed to separate downgoing direct arrivals from upgoing reflections after or before removing those unwanted waves and noises. Since in a depth-time domain (of a shot or receiver gather), the downgoing direct arrival has an opposite apparent dip to those of upgoing reflected events, separation can be easily done by designing a dip filter in an f - k transformation domain (Hardage, 1983). An alternative to this method is to use a median filter (Hardage, 1983; Stewart, 1985).

Crosswell seismic data, however, contain a more complex wavefield than do VSP data. Unlike VSP data, crosswell data contain not only downgoing direct arrival, but upgoing direct arrival as well. Downgoing reflections, which are thought of as unwanted waves in VSP data simply because they are formed by multiples, are no longer unwanted waves in the crosswell case. On the contrary, they are useful signals for crosswell reflection imaging. Furthermore, both downgoing and upgoing reflections are interfered with direct waves in crosswell data more severely than in VSP data. To remove crosswell direct waves and separate upgoing and downgoing reflections, the use of an f - k velocity filter or median filter was suggested by Baker and Harris (1984), Iverson (1988), and Abdalla et al. (1990). Abdalla et al. (1990) separated these events also by muting.

In fact, the potential of separation of crosswell reflections from direct arrivals can be exploited by multi-domain gathering of the data. In this study, we remove direct arrivals in common-interval gathers by using a median filter and perform upgoing and downgoing reflection separation in shot or receiver gathers by using an f - k filter.

Direct arrival removal

We have known from the previous discussion that, in the case of constant-velocity medium, crosswell direct arrivals are already flat in common-interval gathers (as shown in Figure 5). This characteristic enables us to use a median filter to remove them from the total wavefield. Therefore in this case, picking and time shifting direct

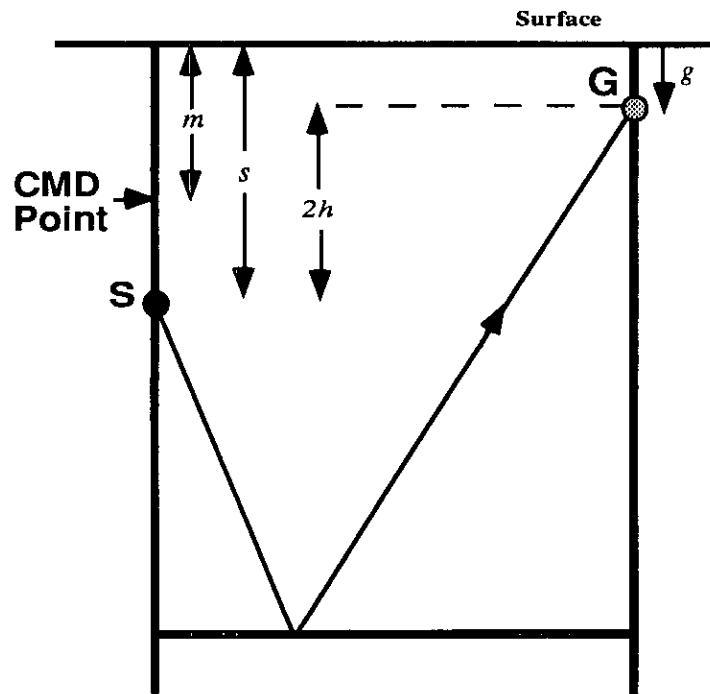


FIG. 7. Relationship among the coordinates used in crosswell geometry. s is source depth, g is receiver depth. Common mid-depth is given by $m=(s+g)/2$, and half of common interval is $h=(s-g)/2$.

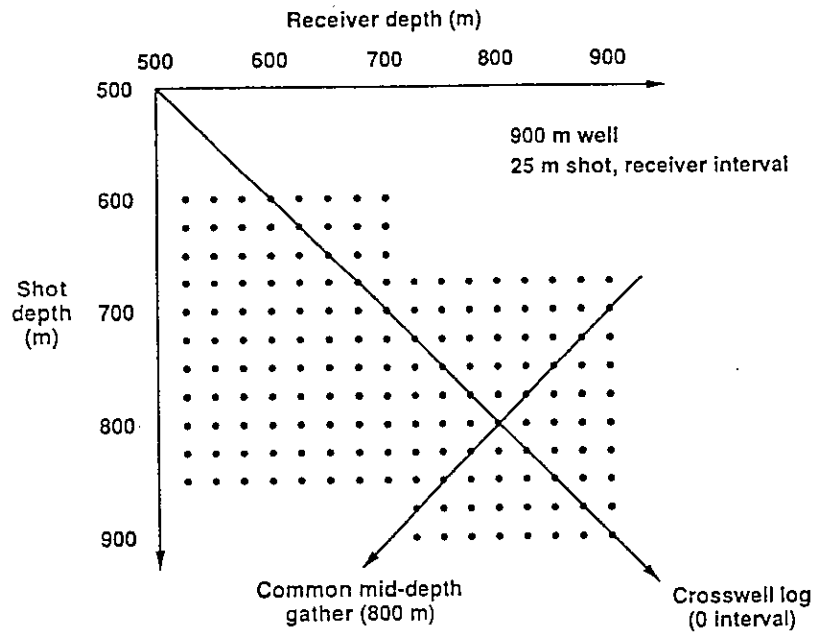


FIG. 8. Crosswell stacking chart (after Stewart, 1991)

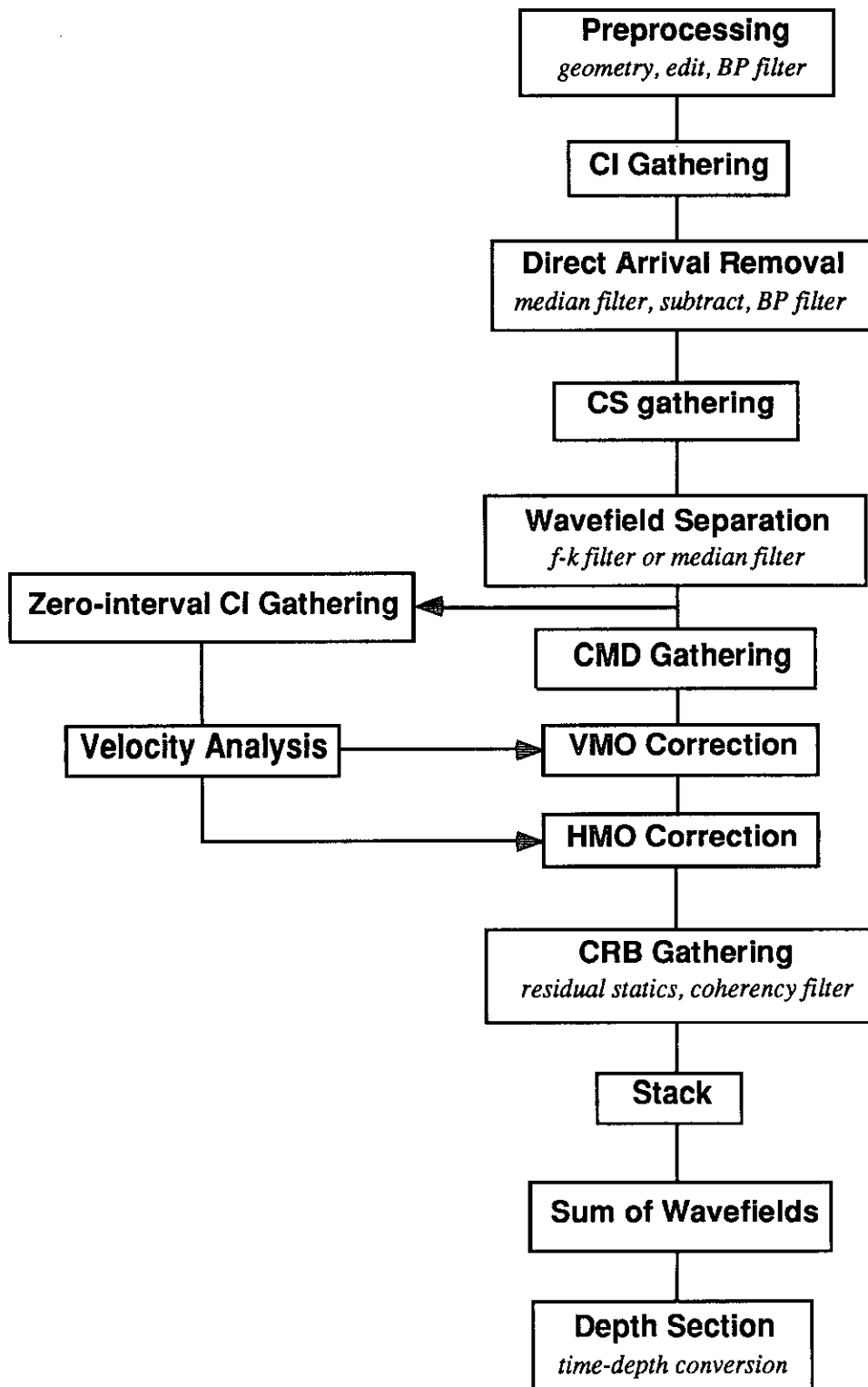


FIG. 9. Processing flow for crosswell reflection imaging.

arrivals in shot records becomes unnecessary. Figure 10 shows the result of data shown in Figure 5 after applying a median filter whose operator length is 11 traces. The direct wave event in each of the CI gathers has been enhanced. They are then subtracted from the total wavefield in original CI gathers of Figure 5. This subtraction yields CI gathers with only reflections retained (Figure 11). By comparing Figure 11 with Figure 5, it can be seen that the direct arrivals have been removed very nicely. Notice that the effect of high frequency glitch noise caused by median filtering appears in the filtered data (Figure 11). These glitches may be taken away by applying a bandpass filter (Stewart, 1985).

Upgoing and downgoing reflection separation

After the direct arrivals have been removed, the filtered CI gathered data are sorted back into CS gathers. An f-k filter could have been applied to the filtered CI gathers in order to separate the upgoing and downgoing reflections. This is because in such gathers these reflections have opposite apparent dips, which is an advantage taken by the f-k dip filter. However, we have noticed that as the vertical source-receiver interval becomes larger, traces contained in CI gathers become less. Due to this, the effect of f-k dip filtering would be less obvious, if applied to gathers with too few traces. Therefore, it is not recommended to separate reflections in these gathers; instead, a common-shot gather (or a common-receiver gather) is a right domain in which to perform reflection separation.

Figure 12 shows reflection data that have been sorted back to CS gathers. Multichannel velocity filters can be used. We used an f-k filter. Median filtering could also be used but involves time-consuming event picking. After the upgoing and downgoing reflections are separated, the data will be ready for further processing.

VELOCITY ANALYSIS AND MOVEOUT CORRECTIONS

Further processing leading to final imaging is performed in CMD gathers. This is because reflected waves in this domain are flat events. This is very similar to the case of conventional surface seismic data processing where all reflections in CDP gathers are flattened after normal moveout corrections. However, things in the crosswell case are somewhat different. First, in a CDP gather, the flattened reflections are from the same depth points on flat reflectors, thus traces can be summed to give a stacked trace. In a CMD gather, reflections are from different depth points even when reflectors at depth are flat. Second, although reflections in a CMD gather are flat, no moveout has been corrected yet. Apparently, crosswell processing cannot exactly follow the CDP processing.

The reflection data are transformed from CS gathers into CMD gathers. Figure 13 shows the separated upgoing reflection. Before imaging can be done, both upgoing and downgoing reflections, which have been separated, must be corrected for moveouts. The moveouts to be corrected include horizontal moveout (HMO) and vertical moveout (VMO). HMO refers to the moveout caused by the separation distance between the source well and the receiver well, which is constant in most crosswell surveys. VMO represents the moveout due to the depth differences between CMD gathers. We want to correct these moveouts in a time domain. However, the moveouts both are a function of distance. Therefore velocity information must be known in order to make such corrections in terms of traveltimes. Velocity information is obtained from

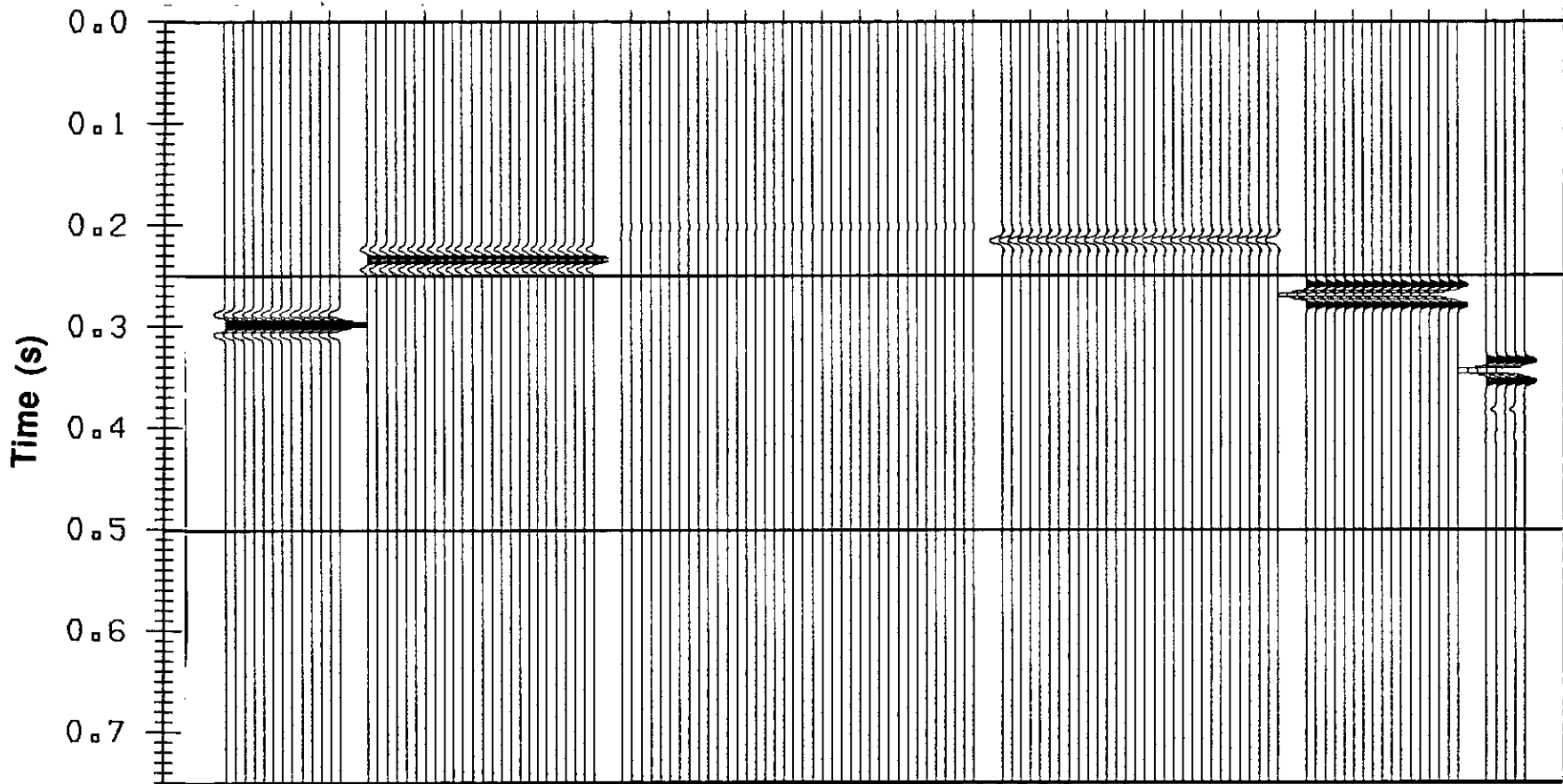


FIG. 10. Direct arrivals removed from common interval gathers in FIG. 5 after applying a median filter. The filter operator is 11 traces long.

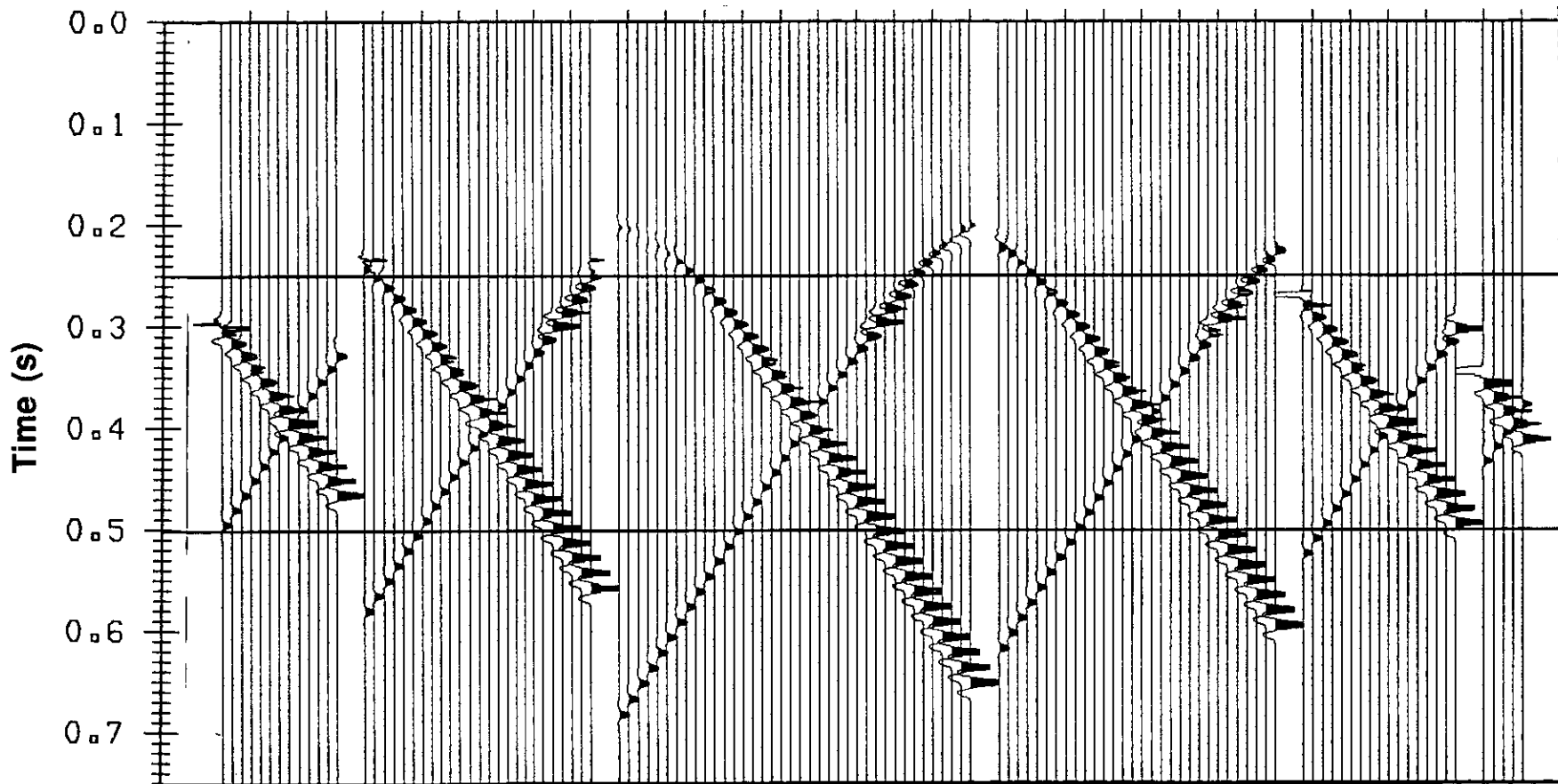


FIG. 11. Common interval gathers after removing direct arrivals. Median filtering works very well in filtering out direct arrival. Note the high-frequency noise (glitches) generated by median filtering.

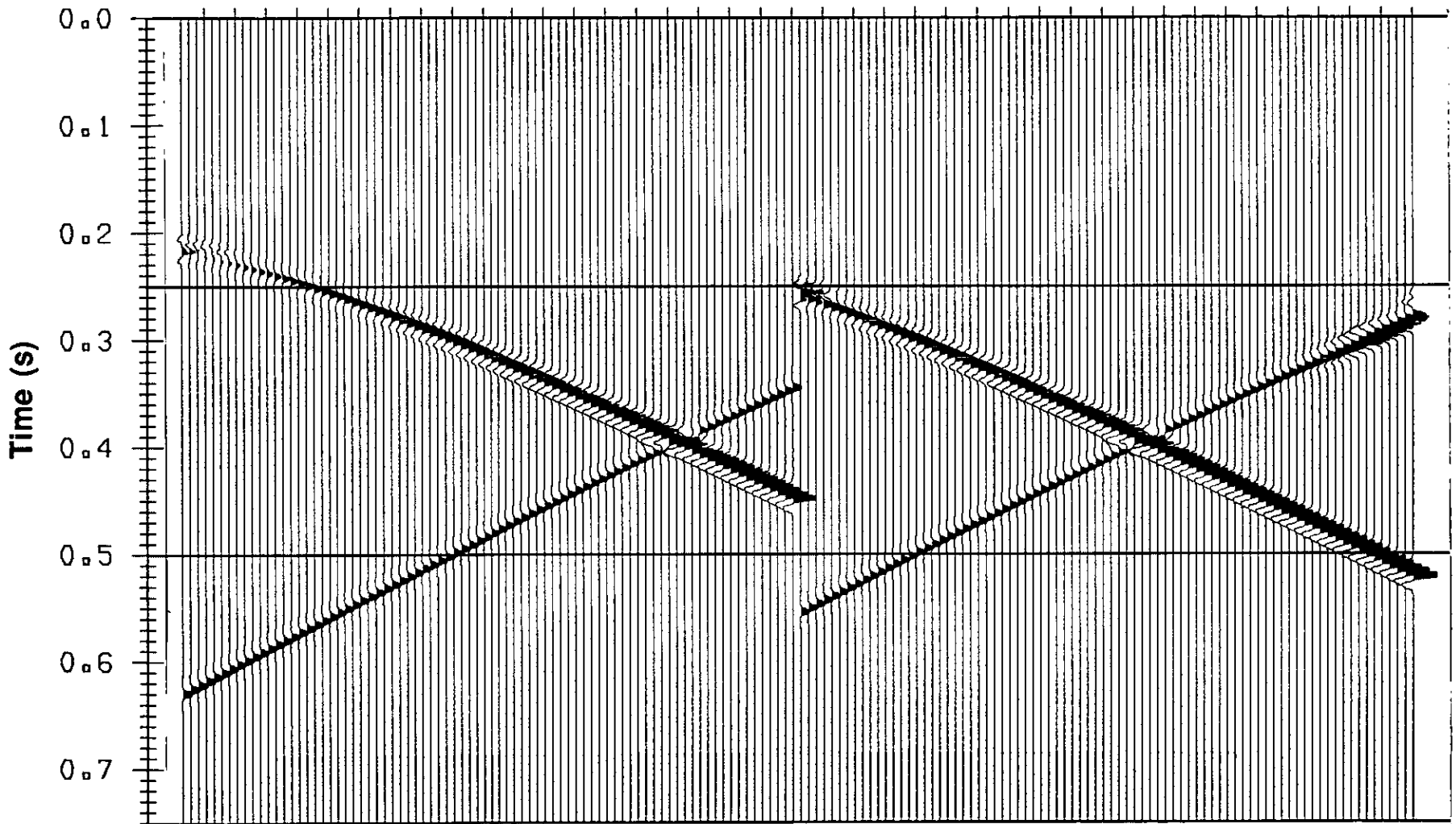


FIG. 12. The same common shot gathers as in FIG. 2, but after direct arrivals have been removed.

velocity scanning analysis in a zero-interval (or offset) CI domain, while VMO and HMO corrections are carried out in CMD domains, as discussed in the following.

Zero-interval velocity analysis

A zero-interval gather is a collection of traces whose vertical interval (or offset) between the source and the receiver for each trace is the same and equal to zero. In fact, a zero-interval gather is a special case of a CI gather. Figure 14 is a zero-interval gather where both upgoing and downgoing reflections are displayed together, although using only one of them is sufficient to derive velocity information from the gather.

We consider a constant-velocity medium in which reflectors are flat. Figure 15a shows a few raypaths of reflections from a flat reflector in such a medium, and Figure 15b gives the corresponding traces in a zero-interval gather. It is noted that all these reflections are from the same reflecting point in the case we are considering, and that there is a moveout between traces. What is to be done is to remove these moveouts, which are VMOs according to our definition, and adjust each trace to a reference time.

Look at Figure 15a again. We find that the interval between adjacent traces actually is the difference between two adjacent CMD depths. Obviously, the moveout, Δt , is a function of CMD depth, velocity and a reference time. This can be formulated as follows.

The traveltime, t , for a particular upgoing reflection recorded at depth Z is given by

$$(1) \quad t = \frac{2}{V} \left\{ \left(\frac{X}{2} \right)^2 + (D-Z)^2 \right\}^{1/2},$$

where V is the medium velocity, X is well-to-well distance and D is the depth of the reflector. V and D are unknowns. So the moveout for the reflection recorded at Z , with respect to the reference time, t_r , is

$$(2) \quad \Delta t = t - t_r.$$

The reference time t_r can be arbitrarily chosen. Hence, we choose, as the reference time, the known traveltime of the reflection from the first trace (at depth Z_1) in the zero-offset gather, that is,

$$(3) \quad t_r = \frac{2}{V} \left\{ \left(\frac{X}{2} \right)^2 + (D-Z_1)^2 \right\}^{1/2},$$

from which, the reflector depth D can be solved for:

$$(4) \quad D = \left\{ \left(\frac{V t_r}{2} \right)^2 - \left(\frac{X}{2} \right)^2 \right\}^{1/2} + Z_1.$$

Now after substitutions, we obtain a unified formula for VMO correction in zero-interval gather:

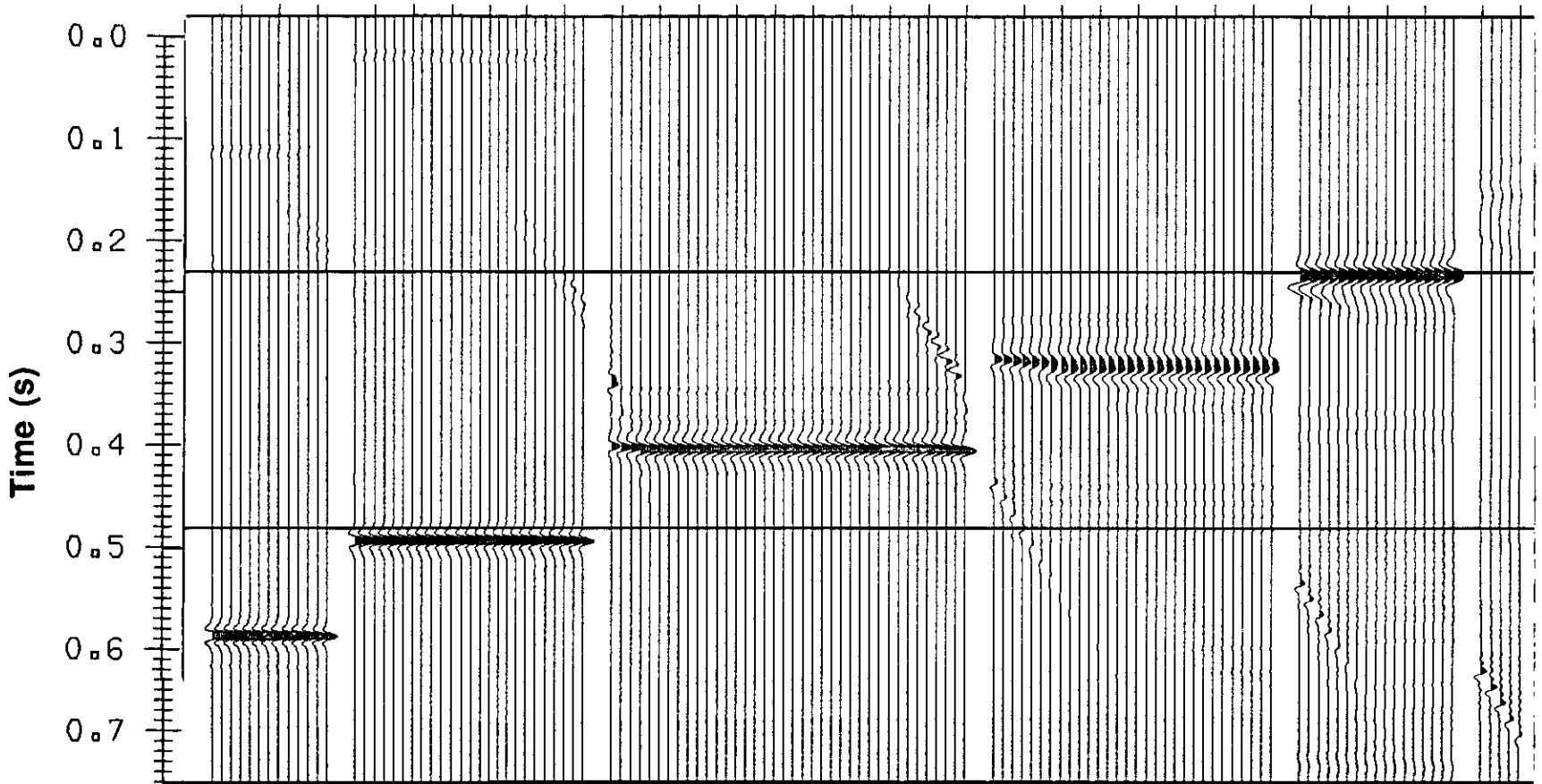


FIG. 13. Upgoing reflections in common mid-depth gathers.

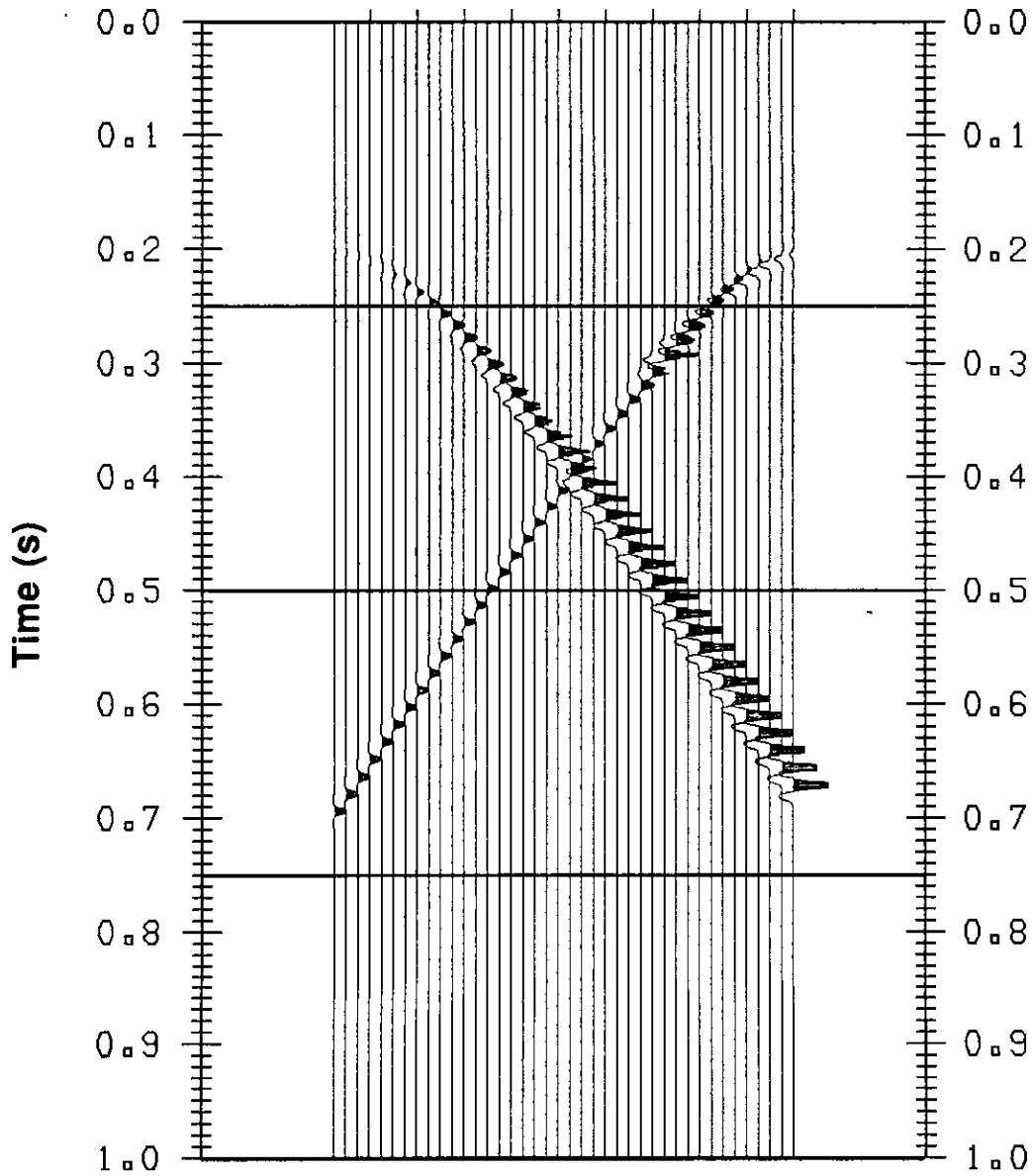


FIG. 14. A zero-interval CI gather used to derive moveout correction velocities. Here both upgoing (right-down-to-left) and downgoing (left-down-to-right) reflections are shown.

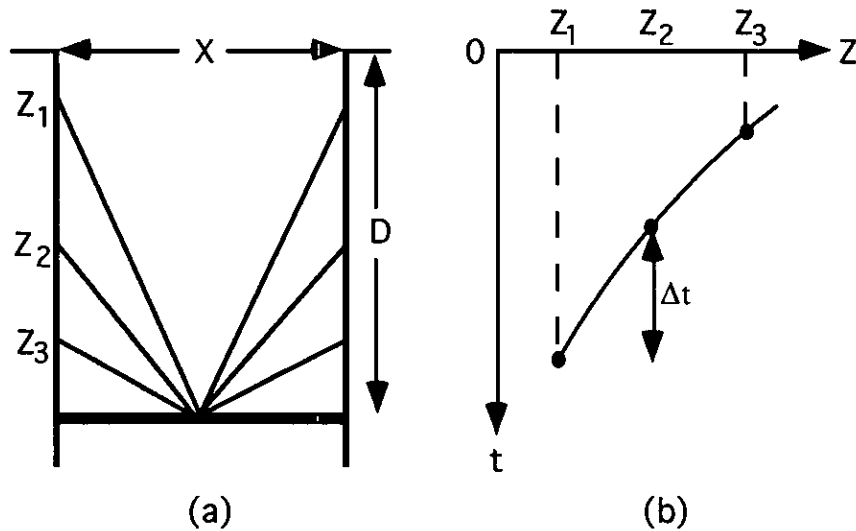


FIG. 15. (a) Raypaths for upgoing reflections in a zero-interval gather. (b) A time-depth representation for the zero-interval gather.

$$(5) \quad \Delta t = \frac{2}{V} \left\{ \left(\frac{X}{2} \right)^2 + \left[\sqrt{\left(\frac{V t_r}{2} \right)^2 - \left(\frac{X}{2} \right)^2} + Z_1 - Z \right]^2 \right\}^{1/2} - t_r$$

It can be seen that the moveout is a function of medium velocity V only. The moveout correction is a process of mapping data from domain (t, Z) into domain (t_r, Z) . We scan a range of possible velocities so that the best velocity can be selected. This best velocity should allow the concerned reflection event in the gather to be best flattened. This process is illustrated in Figure 16, where the original gather is plotted together with six gathers after VMO correction is performed with different scanned velocities. The event to be moveout corrected is the reflection right-down-to-left in the original gather. Notice that this event has some change in wave shape from trace to trace for the last portion of the data, due to phase change in synthetic data generation for the reason we have explained. From the moveout corrected gathers, we can see that the reflection event in the middle gather has been best corrected. This gather corresponds to a velocity of 2500 m/s, which is exactly the medium velocity we used. Actually this is expected by the theory. The same reflection event in all other gathers, corrected with velocities different than the desired velocity, is seen to be either under-corrected or over-corrected just because of incorrect velocities used. Therefore the velocity analysis in zero-interval gather by virtue of velocity scan works reasonably well. The velocity derived this way will be used in the following moveout corrections.

Vertical moveout correction

The problem of VMO correction can be expressed by diagrams in Figure 17. Two shadowed columns in the diagram at the lower left corner represent two CMD gathers. The two horizontal bars denote the flat reflections (upgoing in this case), from the same reflector. Because there are depth differences among CMD gathers, the reflection event from the same reflector in each gather exhibits a traveltime shift (VMO). VMO correction is to remove the moveout and relocate the reflection event according to

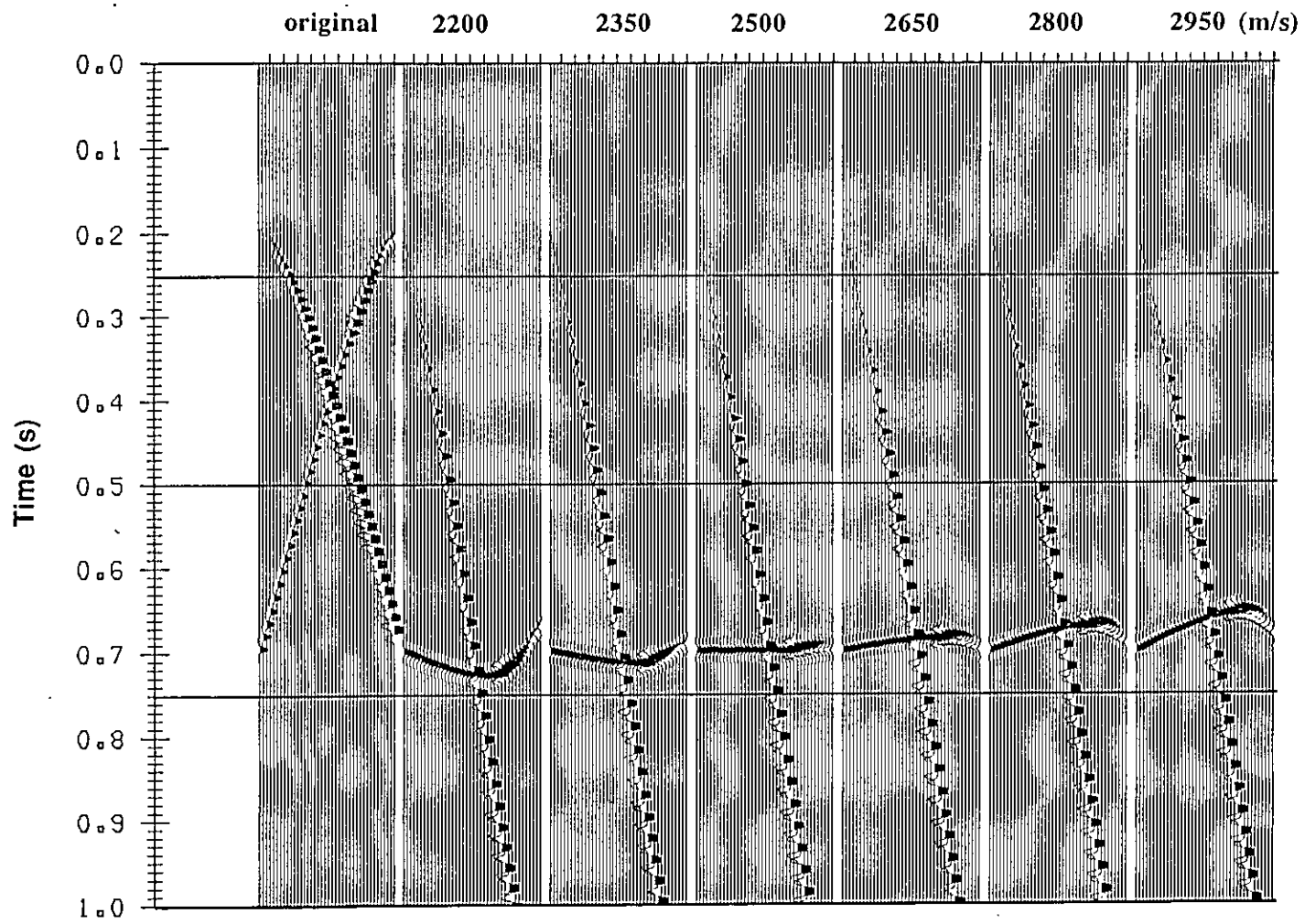


FIG. 16. Velocity scan of a zero-interval CI gather.

a reference time, as shown in the lower right diagram. A VMO equation is developed from equation (5) and given by

$$(6) \quad t_m^2 = t_r^2 + \frac{4(m-m_r)^2}{V_{VMO}^2} - \frac{4(m-m_r)}{V_{VMO}} \sqrt{t_r^2 \left(\frac{X}{V_{VMO}} \right)^2}$$

t_m is the travelttime of the reflection in a CMD gather at CMD depth m . t_r is the reference time corresponding to CMD depth m_r . VMO velocity has been derived from zero-interval gather velocity scanning discussed above. It can be seen that time t_m is a function of CMD depth difference $m-m_r$. A graph in Figure 18 shows this relationship. Stewart (1991) performed VMO corrections assuming a linear VMO vs CMD depth relationship. But this is valid only when CMD depth is not large enough. When CMD depth is very large, the curve in Figure 18 becomes nonlinear.

The reflection data in Figure 13 are VMO corrected. The result is shown in Figure 19. Here a VMO velocity of 2500 m/s was used, and the reference time was selected at the reflection time in the CMD gather corresponding to the shallowest CMD depth. It is seen that the upgoing reflection from the same deep reflector in the earth model (Figure 3) in each CMD gather has been corrected to the same level. The same process can be applied to the CMD gathers which carry downgoing reflection data.

Horizontal moveout correction

To this point, the effect of HMO (due to well separation distance) still exists in the reflection data, and it has to be corrected. The expression for HMO moveout is simple:

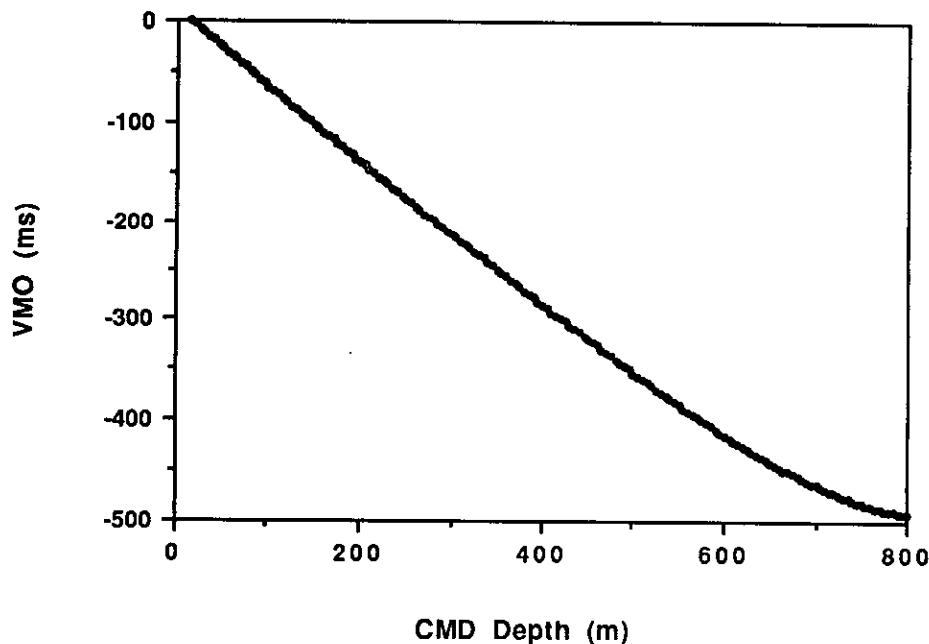
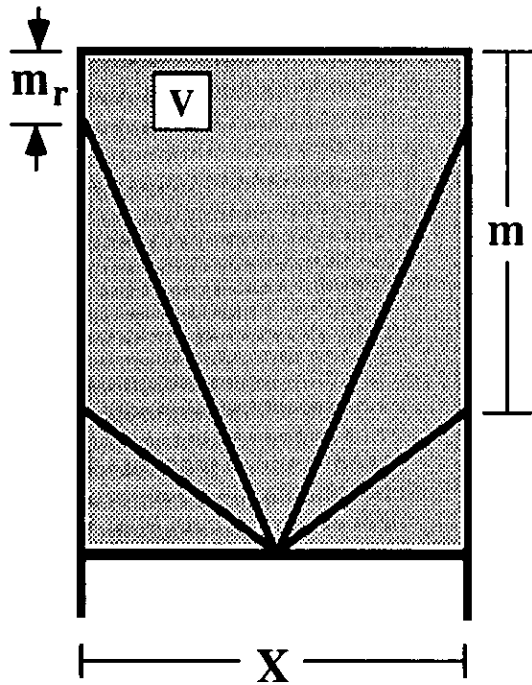


FIG. 18 Dependence of vertical moveout upon common mid-depth.



VMO Equation

$$t_m^2 = t_r^2 + \frac{4(m - m_r)^2}{V_{VMO}^2} - \frac{4(m - m_r)}{V_{VMO}} \times \sqrt{t_r^2 - \left(\frac{X}{V_{NMO}}\right)^2}$$

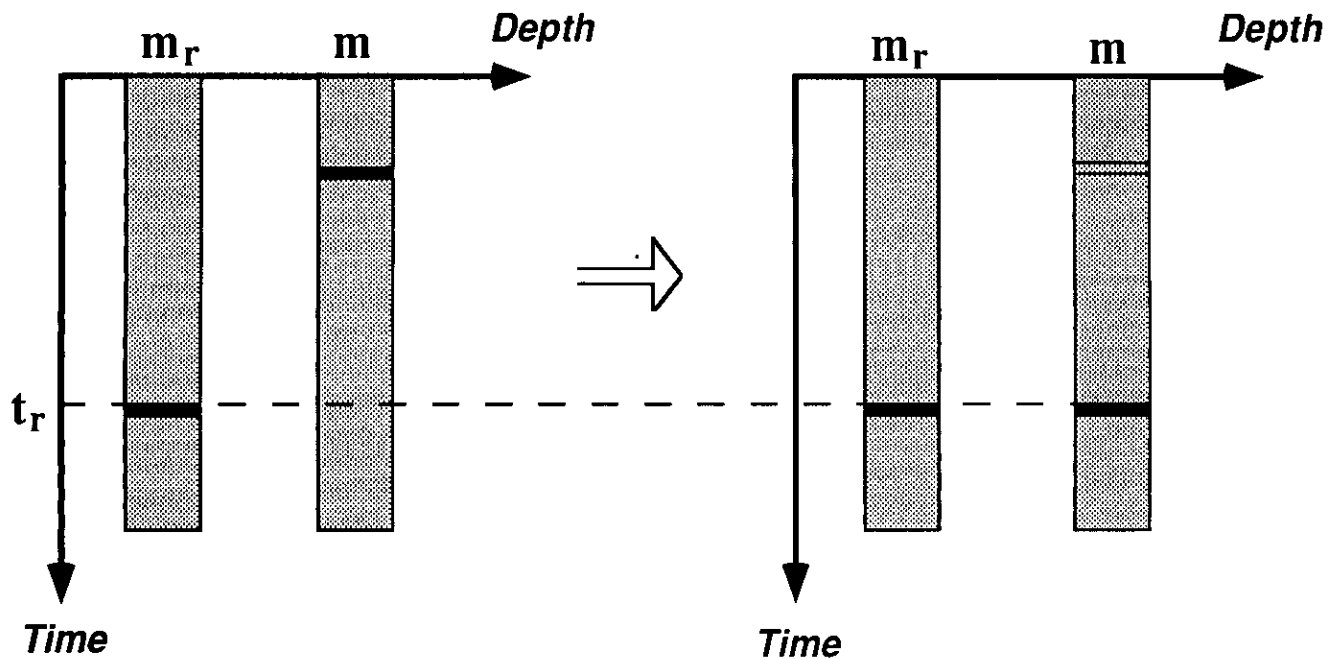


FIG. 17. Diagrams illustrating the process of VMO correction.

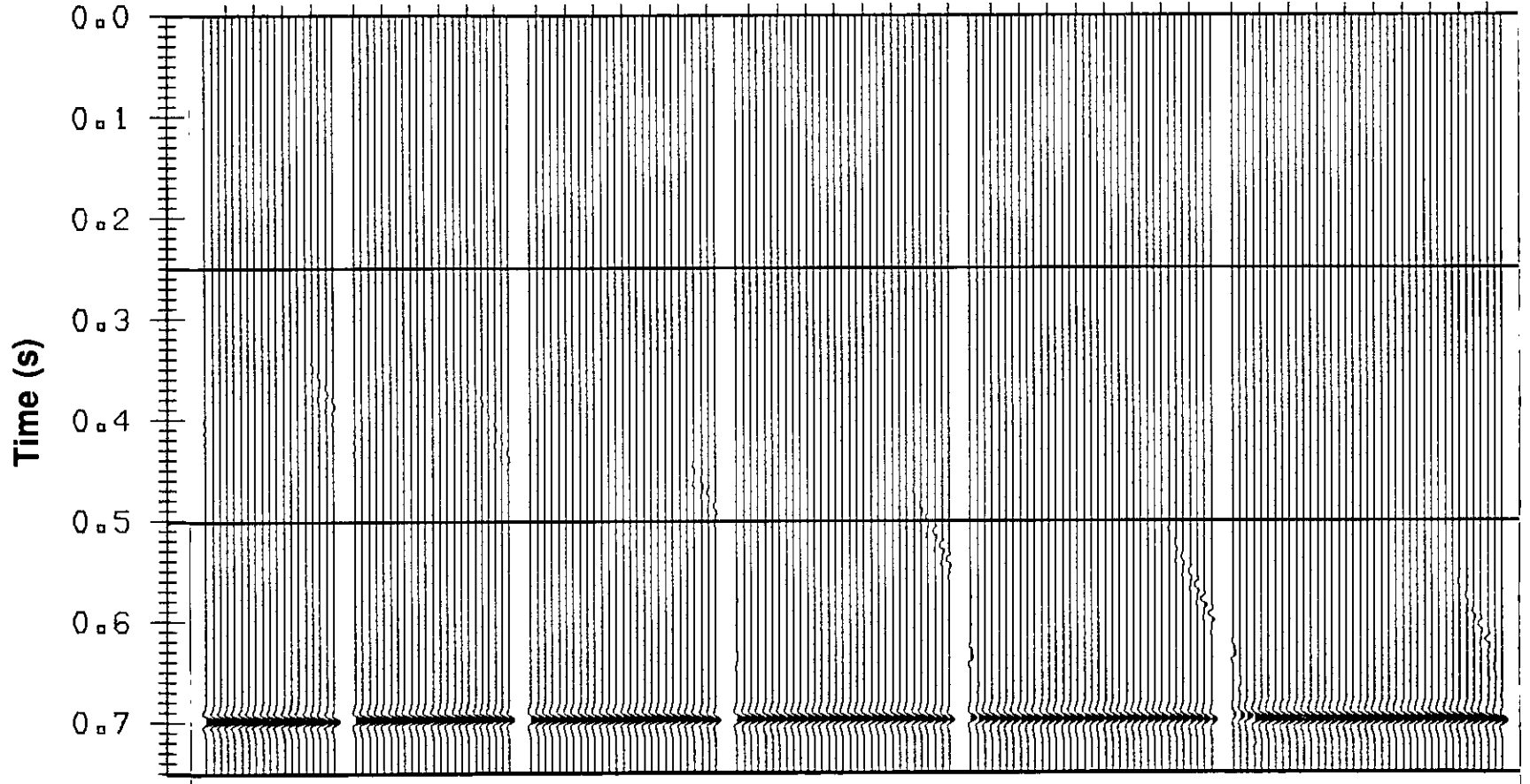


FIG. 19. Upgoing reflections in CMD gathers after vertical moveout is corrected.

$$(7) \quad t_r^2 = t_0^2 + \frac{X^2}{V_{HMO}^2} ,$$

where t_r is the reference time in the VMO corrected CMD gathers, t_0 is two-way vertical traveltime, and V_{HMO} is HMO velocity and here set to be equal to the medium velocity in the constant-velocity medium case. To correct for HMO moveouts, mapping from domain (t_r, z) to domain (t_0, z) must be performed. This process was applied to the data in Figure 19.

CRB GATHERING, STACK AND IMAGING

Crosswell reflection data in a CMD gather represent the energy reflected back from different lateral positions on the reflectors, even after VMO and HMO corrections are done. So, in order to stack the reflection data, traces need to be ordered across all CMD gathers in such a manner that their reflection points are located in the correct lateral positions. One best way probably is that common-reflection points are found according to which all traces are re-ordered. To ensure sufficient fold in the re-ordered gathers, we use common reflection bins (CRB) to replace common reflection points. The bin size is selected depending on the trace fold desired. Reflection data in CRB gathers will be summed to yield a stacked section. Detailed discussion is given in the following two subsections.

CRB gathers

Figure 20 schematically shows the lateral location of reflection points. In a constant-velocity medium, the lateral dispersal of the reflection points from the point half way between wells is given by

$$(8) \quad \Delta X = \frac{X}{4} \frac{s-g}{D-m} ,$$

where s and g are depths of the source and receiver, respectively. D is the depth of a flat target reflector. m is the CMD depth. The depth, D , of a certain target reflector can be found through equation (4). According to equation (8), the location of reflection point for every trace in the data set can be found. But to ensure that we have enough traces when stacking, we divide the range to be imaged into various bins. Traces that fall into the same bins are collected into common reflection bin (CRB) gathers. By doing so, we assign each trace to its correct lateral reflection position.

Four CRB gathers for upgoing reflection data are shown in Figure 21. A bin size of 5 m was used. The reflection arrivals in each gather are from the same reflection bins, thus they can be summed horizontally. Note some changes in waveform for those traces on the right side of each gather. These changes are due to phase change of waves in ray tracing, as we mentioned before. The bin numbers in the figure are counted from the source well. The first bin is 5 m away from the well. As should be expected, the gathers from the middle bins have higher folds.

Stacking and Imaging

Once all the traces are grouped into CRB gathers, a horizontal stacking can be performed. Summing traces in a CRB gather yields a stacked trace. A stack section

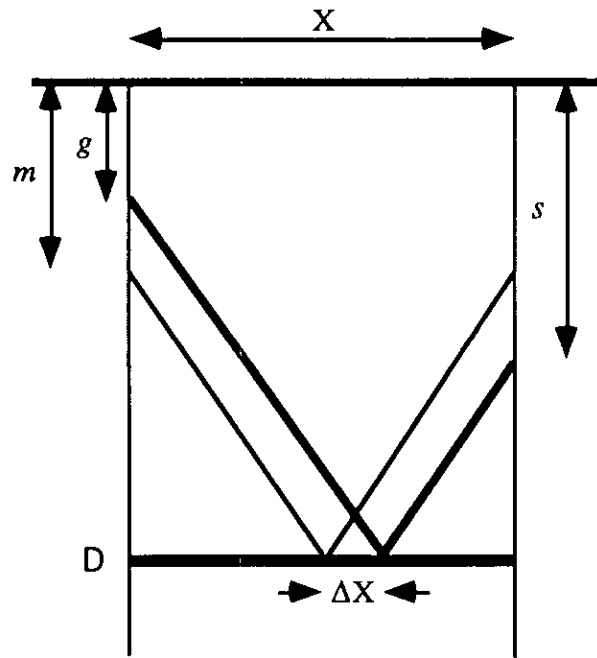


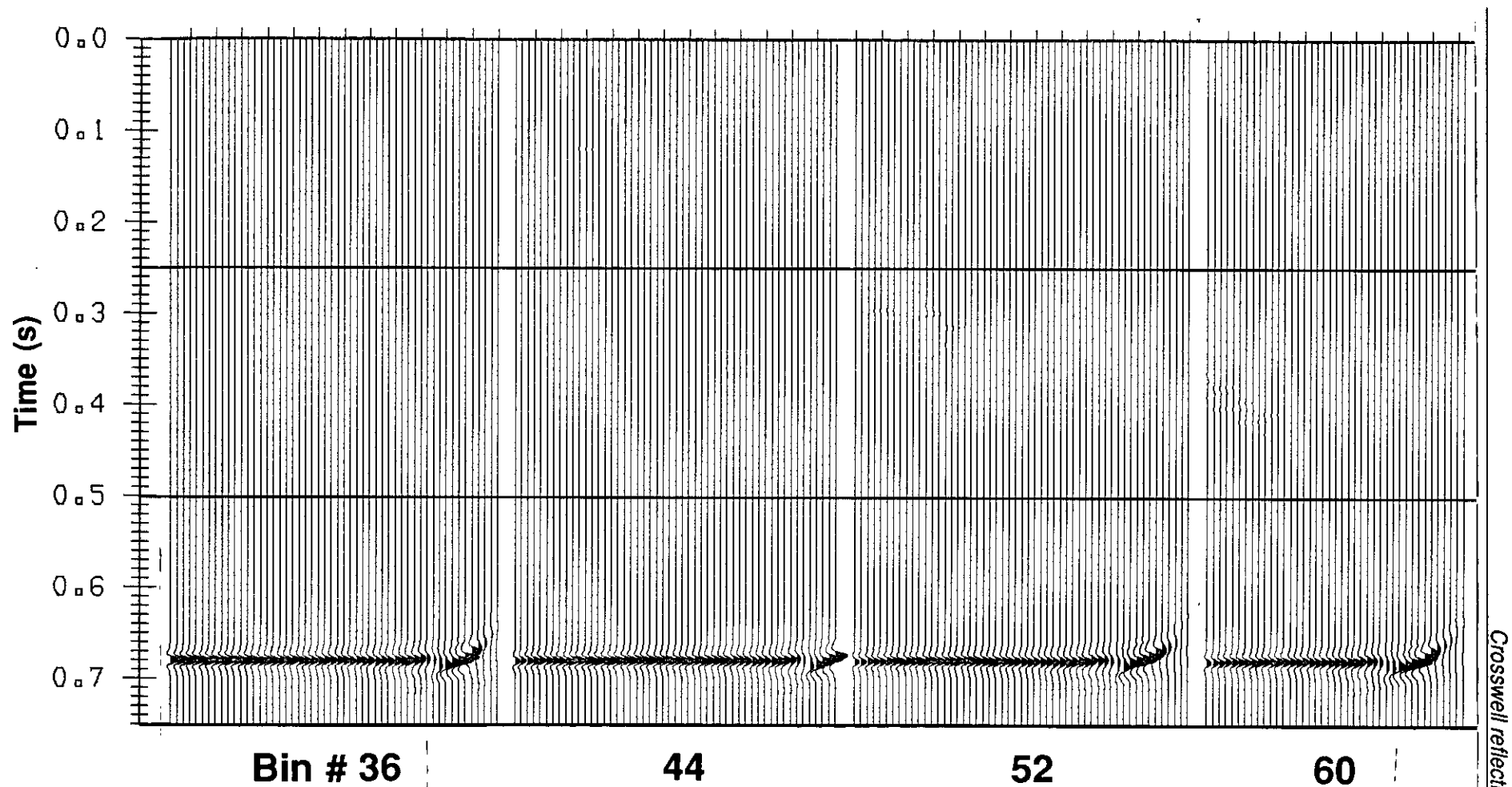
FIG. 20. Diagram showing the lateral position of reflecting points.

is thus generated. Since we deal with the upgoing and downgoing reflection wavefields separately, we will have two stack sections. These two sections should be combined to result in a final stack section. Figure 22 shows such a stack section, resulting from the imaging process we described above. Because HMO corrections have been done, the traveltimes are two-way vertical times. On this section, we see two reflection events. The upper one is the reflection from the surface reflector in our model, whereas the lower event represents the deep reflector. Both are well imaged. It should be noted that a significant lateral coverage of the reflectors by our crosswell reflection imaging procedure is achieved. The reflectors in our model are both 500 m wide. From Figure 22, a majority portion of the upper reflector (the surface), about 480 m wide, is reconstructed by reflection imaging. The lower reflector that we can see through the reconstructed image is about 445 m wide. Therefore, the crosswell reflection imaging procedure generates a fairly good result. A stack section which has no HMO corrected is also shown in Figure 23 for comparison.

A depth section can be obtained if time-depth conversion is carried out. The depth section will give an actual representation of the depth model. We do not discuss the time-depth conversion here.

CONCLUSIONS

We have analyzed in detail a procedure of crosswell seismic reflection processing based on using multiple data domains which include common-shot (or receiver), common-interval, and common-mid-depth gathers. We have shown the effectiveness of the method with an example crosswell data set numerically generated



Crosswell reflection imaging

FIG. 21. Resorted crosswell upgoing reflection data according to common reflection bins. Bin size used is 5 m. Waveform changes seen on the right side of each gather are due to phase changes of waveforms in ray tracing. Bin numbers are counted from the source well.

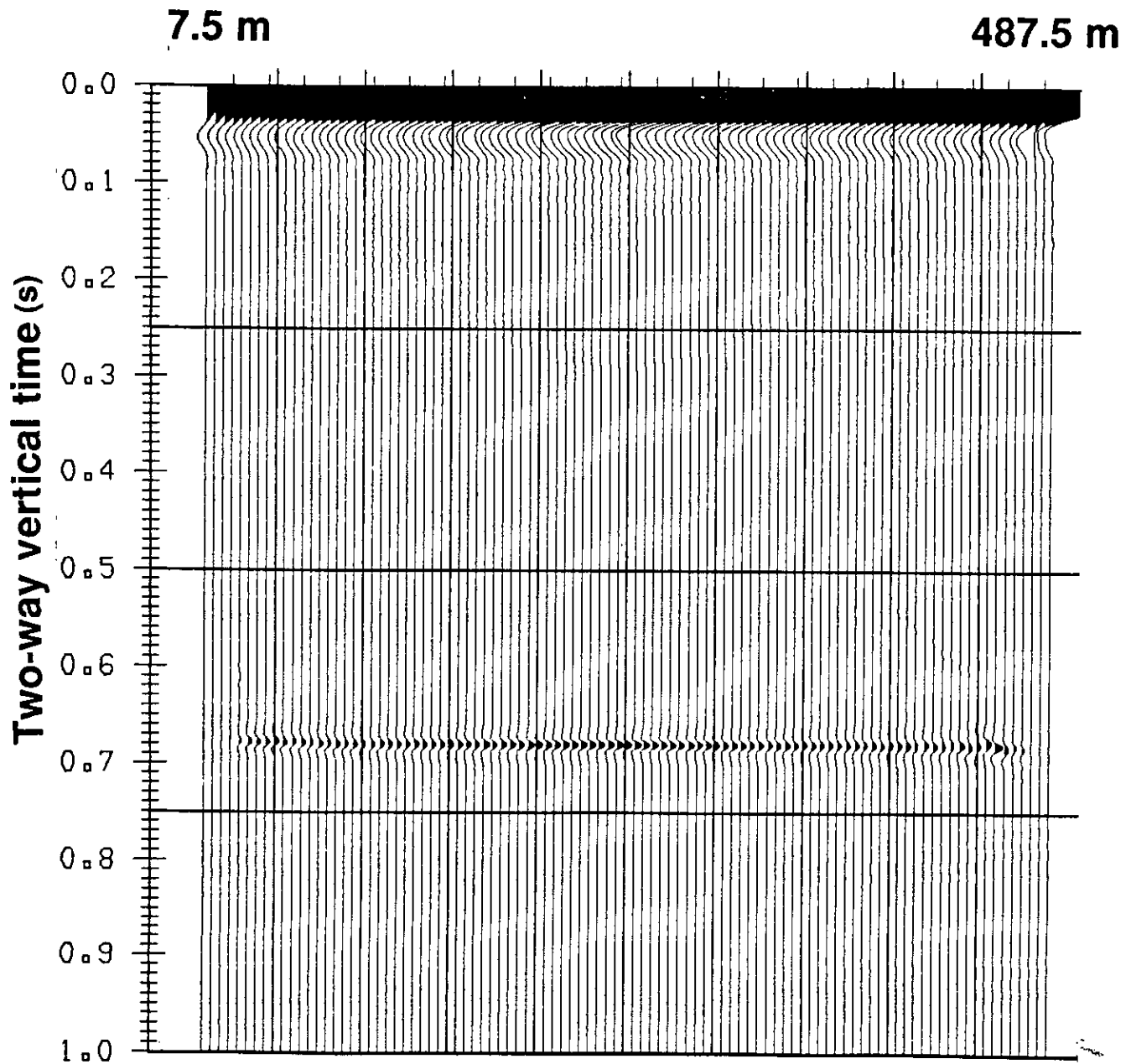


FIG. 22. Final stack section from crosswell reflection imaging. Both the surface reflector and the deep reflector in the earth model in FIG. 1 has been imaged. Note the lateral coverage brought by the imaging procedure. The reflectors between wells are 500 m wide. About 480 m of the upper reflector and about 445 m of the lower reflector have been well imaged.

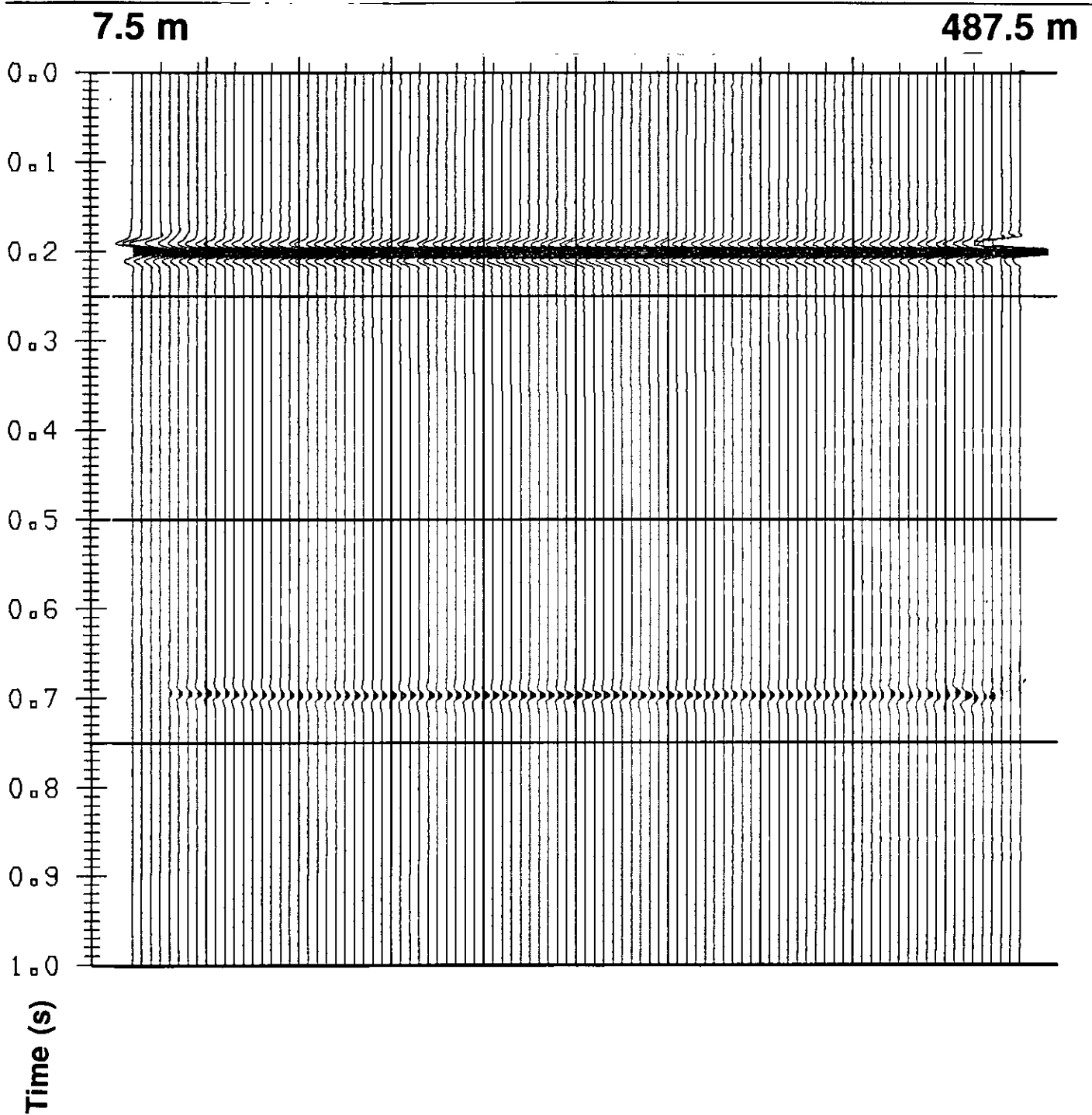


FIG. 23. Final stack section as in FIG. 22, but without horizontal moveout correction applied.

from a constant-velocity medium. The reflector we considered here is flat. In this case, direct arrival waves can be easily removed from the common-interval gathers; both upgoing and downgoing reflections are flat in common-mid-depth gathers. After horizontal and vertical moveout corrections, the flat reflections in common-mid-depth gathers are gathered into common-reflection-bin gathers, in which traces are summed to give a stacked trace. The stacked section obtained this way represents an image of the subsurface reflectors. This whole procedure can be implemented without much difficulty for the case we considered. Although the earth model we used here is a simple one, it allows us to develop some ideas of processing and imaging crosswell reflection data. Some of the ideas presented perhaps can be used for a more complex medium case.

FUTURE WORK

We have so far considered a constant-velocity medium in which reflectors are flat. The processing methods for crosswell seismic reflection data have been developed for this simple case. Although these methods generally work very well for the simple case, they encounter problems when used for complex cases.

The complex cases include multiple dipping layers in a constant-velocity medium, multiple flat layers in varying velocity medium, dipping layers in variable velocity medium, and so on. Processing methods are necessary to develop for these cases if we need to process real crosswell seismic reflection data. The problems we have found so far are those of velocity determination, reflection point determination, pre-stack migration, and dip moveout. Some of them will be considered in future work.

ACKNOWLEDGMENT

The work is supported by the Consortium for Research in Elastic Wave Exploration Seismology (the CREWES Project) at the University of Calgary. The authors wish to thank sponsors of the CREWES Project for continuous support.

REFERENCES

- Abdalla, A. A., Stewart, R. R., and Henley, D. C., 1990, Traveltime inversion and reflection processing of cross-hole seismic data: Presented at the 60th SEG Intern. Ann. Mtg.
- Baker, L. J., and Harris, J. M., 1984, Cross-borehole seismic imaging: Presented at the 54th SEG Intern. Ann. Mtg.
- Hardage, B. A., 1983, Vertical Seismic Profiling, Part A: Principles, Geophysical Press, Amsterdam.
- Iverson, W. P., 1988, Crosswell logging for acoustic impedance: *Journal of Petroleum Technology*, January, 75-82.
- Lazaratos, S. K., Rector, J. W., Harris, J. M., and Van Schaack, M., 1991, High-resolution Imaging with cross-well reflection data: Presented at the 61st SEG Intern. Ann. Mtg.
- Li, G., and Stewart, R. R., 1992, Imaging the subsurface using crosswell seismic reflection data: A synthetic study: Presented at the 1992 CSEG Convention, Calgary, Alberta.
- Menke, W., 1984, The resolving power of cross-borehole tomography: *Geophys. Res. Lett.*, **11**, 105-108.
- Stewart, R. R., 1985, Median filtering: review and a new F/K analogue design: *J. Can. Soc. Expl. Geophys.*, **21**, 54-63.
- Stewart, R. R., Marchisio, G., and Li, G., 1991, Crosswell seismic imaging: Fundamentals and a physical modeling study: Presented at the 1991 CSEG Convention, Calgary, Alberta.

- Stewart, R. R., 1991, Exploration seismic tomography: Fundamentals: SEG Short Course.
- Stewart, R. R., and Marchisio, G., 1991, Cross-well seismic imaging using reflections: Presented at the 61st SEG Intern. Ann. Mtg.
- Wyatt, K. D., and Wyatt, S. B., 1984, Determining subsurface structure using the vertical seismic profile, in Vertical Seismic Profiling, Part B: Advanced Concepts, edited by M. N. Toksöz and R. R. Stewart, Geophysical Press, Amsterdam.
- Yilmaz, O., 1987, Seismic data processing: Soc. Expl. Geophys.